Electromagnetic Analysis of YBCO Superconducting Cables with High Current Transporting for Electric Devices

H. Zhang, J. Zhu, W. Yuan, M. Qiu, S. Fu, S. Rao, W. Yang and M. Zhang

Abstract— Most high temperature superconducting (HTS) electric devices have been built by employing a superconducting composite cable. These HTS devices generally have large current carrying capacities. Therefore, the electromagnetic characteristic of a composite superconducting cable with high current density becomes a key point for the application of these HTS devices. A helical superconducting cable and a Roebel cable consisted of YBCO coated conductors with the critical current of 500 A @77 K in self-field are both proposed in this paper. The helical superconducting cable has two conductor layers and the structure parameters of the helical cable are given. The Roebel cable has 4 layers with critical current of 500 A. Two 3 D models are built for a helical cable and Roebel cable with variable geometries. Their magnetic flux distributions along the axis are presented based on finite element analysis method and their electromagnetic characteristics are discussed as well. The analysis model can be further applied for the large scale high temperature superconducting electric device design with high current carrying ability.

Index Terms— Helical cable, Roebel cable, magnetic flux distribution, optimal design, 3D FEM.

I. Introduction

RECENTLY, the Yttrium Barium Copper Oxide (YBCO) coated conductor becomes more and more popular for superconducting electric power devices, such as transformers, fault current limiters, energy storage systems, magnets and power transmission cables with high critical current densities of over 3.0 MA/cm^2 in conductor with length exceeding 1 km[1]. HTS devices always require a superconducting cable with high current density when they are placed in a high magnetic field, which decreases the inductances and thus induced voltages during operation at high ramp rates. Helical cable [2,3] and Roebel cable[4] are two kinds of the assembled HTS cables with high current transporting capabilities.

A helical cable consists of copper former and it can improve the stability of the superconductor under quench. But the currents are not uniform in the tapes of helical cable. One the other side, the Roebel cable has uniform current distribution for the full transposition of the tapes. However, Roebel cable has less quench stability compared to the helical cable[3].

In this paper, a helical cable and a Roebel cable are studied. These two kinds of cables with the capability of current transporting 500 A @ 77K is optimal designed based on a full 3D electromagnetic field model using sheet current assumption method. The magnetic flux density distributions of the helical cable along the axis are discussed considering different twist pitches. The magnetic flux density distributions of the Roebel cable are compared as well considering different trapezoidal angles.

This work was support by NSFC Grant 51207146, EPSRC EP/K01496X/1, China State Grid Corporation science and technology project DG71-16-002, RAEng Newton Research Collaboration Programme of UK/NRCP1415134.

H. Zhang, W. Yuan and M. Zhang are with the Department of Electronic and Electrical Engineering, University of Bath, BA2 7AY UK.

J. Zhu, M. Qiu, S. Fu, S. Rao are Department of Electrical Engineering and Novel Material, China Electric Power Research Institute, Beijing, China. W. Yang is with School of Astronautics, Beihang University, Beijing, China

J. Zhu is the corresponding author (Tel: 0086 10 80128056; Fax: 0086 10 80128056; E-mail address: zhujiahui@epri.sgcc.com.cn)

II. Electromagnetic Characteristics Analysis of a Helical Cable

A. Structure introduction of the helical cable

The structure of the helical cable is shown in Fig.1. It mainly consists of a copper former, a conductor layer and an electric insulation layer from inside to outside. The conductor layer is wound with superconducting tapes. The electric insulation layer is usually made of Polypropylene Laminated Paper (PPLP). The winding direction, winding angle β and twist pitch P are main structure parameters of helical cable.

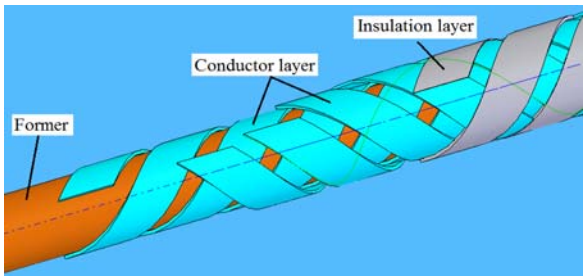

Fig. 1. Structure of a two-layer helical cable with insulation layer on a former conductor.

B. Electromagnetic parameter design

(1) *Self-inductance of the Helical Cable*

Assuming r_0 as the distance between the field point to the axial line, then magnetic field is toroidal when $r_0>r_i$, and it is axial when $r_0<r_i$. Magnetic flux density B of the helical cable is derived with Ampere's law.

$$B_{in} = \frac{\mu_0 I}{P_i} \qquad r_0 < r_i \tag{1}$$

$$B_{out} = \frac{\mu_0 I}{2\pi r} \qquad r_0 > r_i \tag{2}$$

$$P_i = \frac{2\pi r_i}{\tan\beta} \tag{3}$$

where μ_0 refers to permeability of vacuum ($4\pi\times10^{-7}$ H/m), I is the current flowed through the conductor layer, P_i is twist pitch of i^{th} conductor layer, r_i refers to outer radius of i^{th} conductor layer. The self-inductance of i^{th} conductor layer L_i in per unit length is determined by the magnetic field energy W_m (J/m^3). The helical cable has no shielding layer, so the external outer radius is $D=r_i$, and the influence of external magnetic flux density B_{out} does not exist when $r_0>r_i$.

$$W_m = \frac{B^2}{2\mu_0} = \frac{1}{2}\mu_0\frac{\pi r_i^2}{P_i^2}I^2 \tag{4}$$

$$L_i = \mu_0\frac{\pi r_i^2}{P_i^2} = \frac{\mu_0}{4\pi}\tan^2\beta_i \tag{5}$$

(2) *Mutual-inductance of the Helical Cable*

The total magnetic field energy W_m (J/m) between i^{th} and j^{th} conductor layers is:

$$\begin{aligned} W_m &= W_{m1} + W_{m2} + W_{m3} \\ &= \frac{1}{2}L_i I_i^2 + \frac{1}{2}L_j I_j^2 + M_{ij} I_i I_j \end{aligned} \tag{6}$$

where i and j are conductor layers' number (i, j= 1, 2,…). W_{m1} is the magnetic field energy of i^{th} conductor layers; W_{m2} is the magnetic field energy of j^{th} conductor layers; W_{m3} is the magnetic field energy between i^{th} and j^{th} conductor layers.

On the basis of Ampere's law, the total magnetic field energy W_m is derived in (7). The mutual inductance M_{ij} between i^{th} and j^{th} conductor layer of helical cable is given in (8):

$$\begin{aligned} W_m &= \frac{1}{2}\mu_0\frac{\pi r_i^2}{P_i^2}I_i^2 + \frac{1}{2}\mu_0\frac{\pi r_j^2}{P_j^2}I_j^2 \\ &+ \mu_0\frac{\alpha_i\alpha_j}{P_iP_j}\pi r_i^2 I_i I_j \end{aligned} \tag{7}$$

$$M_{ij} = M_{ji} = \mu_0\frac{\alpha_i\alpha_j}{P_iP_j}\pi r_i^2 = \frac{\mu_0}{2\pi}\frac{\alpha_i\alpha_j}{2}\tan\beta_i\tan\beta_j \tag{8}$$

where α_i and α_j respectively refer to the direction of conductor layer(indicated by +1 or -1). When conductor layer is wound on the former by the direction of "Z", the coefficient is -1 and when conductor layer is wound on the former by the direction of "S", then the coefficient is +1.

C. Electromagnetic characteristics analysis of helical cable

Therefore, a helical cable with an outer diameter of 4.6 mm and a critical current of about 500 Ampere @77 K, self-field are designed. The specification of the helical cable is shown in Table I. The electromagnetic parameters of a helical cable consisted of YBCO coated conductors are provided in Table II. The numerical inductance results are based on FEM simulation of the cable and they agree well with the analytical results, which verify the numerical results.

The magnetic flux density of a single HTS tape in the helical cable is shown in Fig. 2. Magnetic flux density in different parts of the helical HTS tape is different. The maximum magnetic flux densities of internal and outer conductor layers are calculated and the varieties of them considering different twist pitch are shown in Fig.3 as well. It can be observed that the axial magnetic flux density B_Z increases when twist pitch varies from 13 mm to 21 mm.

TABLE I
CONFIGURATION OF A 30 CM HELICAL CABLE CONSISTED OF YBCO TAPES

Layers	Structure	Number	Radius
Former	Cross-area	12.56 mm^2	2 mm
Carbon paper	Thickness	0.1	2.1 mm
1st conductor layer	Number of stack	3	2.2 mm
	Direction	-1	
	Pitch	71.24 mm	
	Single wire length	0.305m	
	angle	10^0	
	Total wire length	0.915 m	
2nd conductor layer	Number of stack	3	2.3 mm
	Direction	1	
	Pitch	25.75	
	Single wire length	0.333 m	
	angle	26^0	
	Total wire length	1m	

TABLE II
ELECTROMAGNETIC PARAMETERS OF A 30 CM HELICAL CABLE CONSISTED OF YBCO TAPES

Items	Values
Critical current of 1st layer / A	249.7
Critical current of 2nd layer/ A	250.6
Total Critical current of the cable/ A	500.3
Analytical Self-inductance / μH	0.027
Analytical Mutual inductance /μH	0.017
Numerical Self-inductance / μH	0.028
Numerical Mutual inductance /μH	0.018

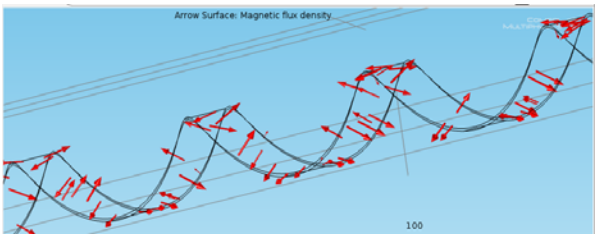

Fig. 2. Magnetic flux density vector distribution of a single tape in helical HTS cable.

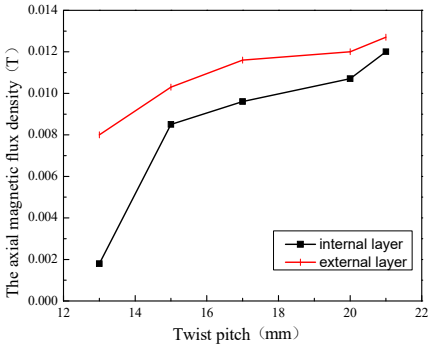

Fig. 3. B_Z distributions of internal layer and external layer with the twist pitch in helical cable. The applied current is 500A.

III. Electromagnetic Characteristics Analysis of a Roebel Cable

A. Structure introduction of the Roebel cable

Roebel cable is another option to increase current-carrying capacity of assembled 2G coated conductors. It is made of meander-shaped YBCO tapes, which are produced by punching out trapezoids from both borders of original conductors. Fig. 4(a) presents the schematic view of a HTS Roebel cable with 4 strands in one pitch length. The transposition of the strands homogenizes the electrical and mechanical properties. This special structure not only decreases the AC loss, but also makes the uniform current distribution. Thus, Roebel cable has attracted considerable interest as one of the high-current cables.

The planar structure of single strand required for Roebel cable are shown in Fig. 4(b). This structure can be described by several geometrical parameters, as shown in Table III[5]. The tape widths (W_R and W_X), trapezoidal angle θ and transposition pitch L are main structure parameters of a Roebel cable. The electromagnetic characteristics of the Roebel cable are influenced by these parameters. This section is focused on discussing the influence of the trapezoidal angle on the electromagnetic behavior. Other parameters will be discussed in the following papers.

(a)

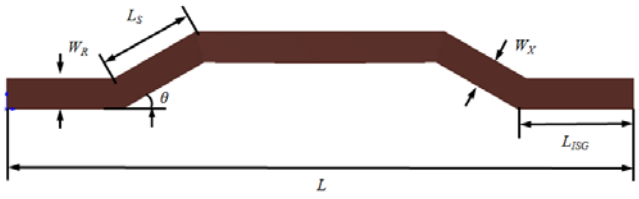

(b)

Fig. 4. (a) The schematic view of an HTS Roebel cable with 4 strands in one pitch length; (b) Shape parameters of one strand.

TABLE III
Paramaters of a Roebel Cable Consisted of YBCO Coated Conductor

Parameter	Name	Roebel I	Roebel II
L	Pitch	80 mm	80 mm
W_R	Strand Width	4 mm	4 mm
W_X	Crossover Width	4 mm	4 mm
L_s	Crossover Length	12 mm	8.48 mm
L_{ISG}	Interstrand Gap	13.7 mm	14.7 mm
θ	Roebel Angle	30°	45°
n	Strand Number	4	4

B. Electromagnetic characteristics analysis of Roebel cable

As shown in Fig. 4(a), the YBCO Roebel cable comprises zigzag-shaped, interlaced strands of coated conductors, the analytical method, which is employed in Section II, cannot be used to calculate the Roebel cable. Therefore, accurate electromagnetic field analysis of such cables can only achieved by finite element simulation with three-dimensional model.

In order to investigate the electromagnetic behaviors, two Roebel cables consisted of YBCO coated conductors are analyzed using COMSOL Multiphysics based on Maxwell theory. If a certain current density J is applied to the section area, the magnetic flux B and magnetic field intensity H can be calculated in (9).

$$\nabla \times B = \mu_0 J \tag{9}$$

Their critical currents are designed as 500 Ampere @77 K, self-field. The specifications of the Roebel cables are shown in Table III. The only differences between these two Roebel cables are the trapezoidal angles: i) Roebel I has the trapezoidal angle of 30°, ii) Roebel II has the angle of 45°.

Since the superconducting layer of YBCO conductor is very thin (usually 1 μm), a thin-strip approximation is used in this simulation, which means the electromagnetic field distribution is uniform along its thickness[6]. Fig. 5 shows the surface current distribution along the single strand.

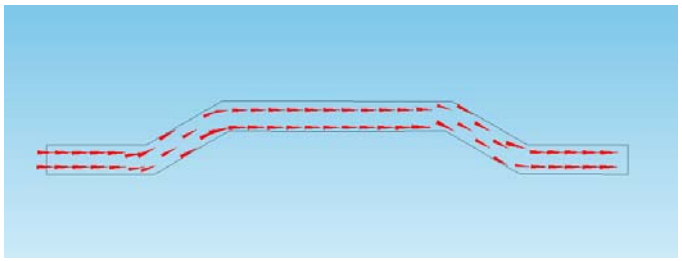

Fig. 5. Current direction of a single HTS coated conductor in Roebel cable.

The magnetic flux density B_Z of single strand in Roebel I is shown in Fig. 6. This strand has the transporting current of 125A. We can find that the magnetic flux density varies in different parts of the Roebel HTS coated conductor. The field along the borders is higher than the middle zone. The magnetic field reaches to peak value at the trapezoidal corner of the strand. The maximum B_Z in the single strand of Roebel I is 21 mT.

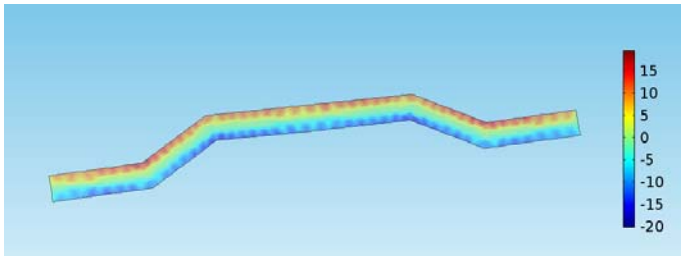

Fig. 6. Magnetic flux density B_Z in single strand of Roebel I. The angle is 30 degree and the applied current is 125A. (Unit is mT)

In order to analyze the trapezoidal angle, the magnetic flux density B_Z of single strand in Roebel II is shown in Fig. 7 with transporting current of 125 A. The maximum B_Z in the single strand of Roebel II is 18 mT, which is smaller than that of Roebel I.

Fig. 8 shows the magnetic flux density B_Z of Roebel I and Roebel II with the transporting current of 500 A. We can find that the maximum magnetic flux density of Roebel I and Roebel II are 36mT and 30 mT respectively, and the trapezoidal angles influence the electromagnetic fields. Although the total current is four times of that in single strand, the magnetic field is only twice of single strand. Moreover, it can be found that the borders of the Roebel cable have higher magnetic field, while the inner borders of the strands have small magnetic fields.

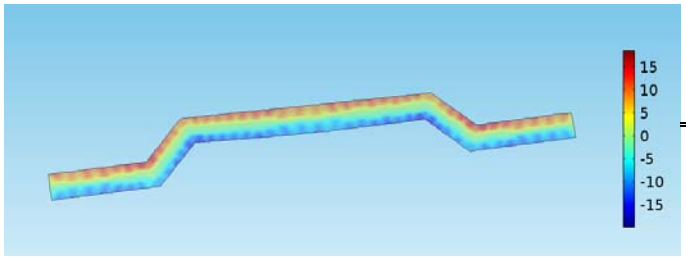

Fig. 7. Magnitude of magnetic flux density in single strand of Roebel II. The angle is 45 degree and the applied current is 125A. (Unit is mT)

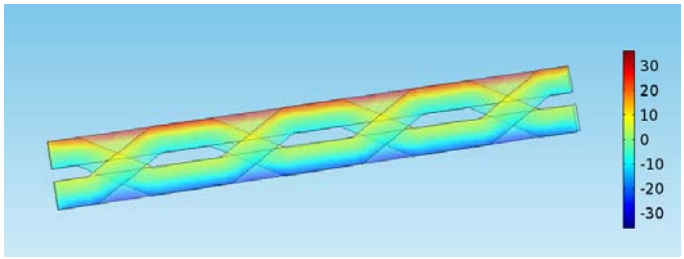

(a)

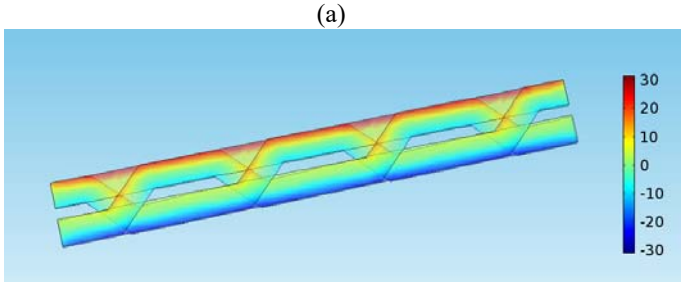

(b)

Fig. 8. Magnetic flux density B_Z when the total applied current is 500A. (a) Roebel I with trapezoidal angle 30°. (b) Roebel II with trapezoidal angle 45°. (Unit is mT)

C. *Electromagnetic parameter design*

The major problem in designing superconducting cable is the calculation of self-inductance and mutual inductance. The inductance of the cable determines the current distribution within different layers. Also, the performances under dynamic conditions are related to the inductance. For regular geometries, such as helical structure, analytical method can be applied in estimation of inductance, as shown in Section II. However, analytical method is not applicable for Roebel configuration due to the weaved zigzag-shaped strands. This subsection aims to calculate the inductance based on FEM results.

The magnetic energy within the circuit can be calculated by

$$W = W_s + W_m = \frac{1}{2} L_s I^2 + MI^2 \quad (10)$$

Where W is the total energy, which can be calculated in COMSOL by integration across the whole space[7]. W_s is the energy in the self inductance. W_m is the energy in the mutual inductance. L_s is the self inductance, which is solved by the simulation results of single strand. M is the mutual inductance. Each strand in Roebel cable transports the same current I. Table IV summarizes the results of energy and inductance.

TABLE IV
ELECTROMAGNETIC PARAMETERS OF A 8 CM ROEBEL CABLE CONSISTED OF YBCO TAPES

Parameter	Roebel I	Roebel II
Applied Current / A	125	125
Energy in Single Strand / J	4.1e-4	4.1e-4
Self-Inductance / H	5.2e-8	5.2e-8
Energy in the Cable / J	4.5e-3	4.5e-3
Mutual Inductance / H	1.84e-7	1.84e-7

IV. CONCLUSION

Electromagnetic analysis of the helical and the Roebel cables using analytical and FEM methods are presented and discussed in this paper. Two 3D models, taking account of variable parameters, are built for helical cable and Roebel cable. The robust numerical models implemented in COMSOL are validated by the analytical results. Finally, the magnetic flux density and inductance with consideration of the different geometries are discussed. These analytical models can be further applied for the large scale high temperature superconducting electric device design with high current transporting. The numerical models are proved to be efficient tools for cables design and can applied in various geometries.

REFERENCES

[1] D. Haught, J. Daley, P. Bakke *et al.*, "Overview of the US Department of Energy (DOE) High‐Temperature Superconductivity Program for Large‐Scale Applications," *International journal of applied ceramic technology,* vol. 4, no. 3, pp. 197-202, 2007.

[2] P. Michael, L. Bromberg, D. van der Laan et al., "Behavior of a high-temperature superconducting conductor on a round core cable at current ramp rates as high as 67.8 kA/s in background field of up to 19 T," *Super. Sci. & Tech.* , vol. 29. no. 4, 045003, 2016

[3] J. Zhu, Z. Zhang, H. Zhang *et al.*, "Electric Measurement of the Critical Current, AC Loss, and Current Distribution of a Prototype HTS Cable," *Applied Superconductivity, IEEE Transactions on,* vol. 24, no. 3, pp. 1-4, 2014.

[4] W. Goldacker, F. Grilli, E. Pardo et al., "Roebel cables from ROECO coated conductors: a one-century-old concept for the superconductivity of the future". *Super. Sci. & Tech.* , vol. 27. no. 9, 093001, 2014

[5] R. A. Badcock, N. J. Long, M. Mulholland *et al.*, "Progress in the manufacture of long length YBCO Roebel cables," *Applied Superconductivity, IEEE Transactions on,* vol. 19, no. 3, pp. 3244-3247, 2009.

[6] M. Nii, N. Amemiya, and T. Nakamura, "Three-dimensional model for numerical electromagnetic field analyses of coated superconductors and its application to Roebel cables," *Superconductor Science and Technology,* vol. 25, no. 9, pp. 095011, 2012.

[7] H. Zhang, Z. Nie, X. Xiao *et al.*, "Design and Simulation of SMES System Using YBCO Tapes for Direct Drive Wave Energy Converters, " *Applied Superconductivity, IEEE Transactions on,* vol. 23, no. 3, pp. 5700704-5700704, 2013.